Realization of Bose-Einstein Condensation with Lithium-7 Atoms

by

Yichao Yu

Submitted to the Department of Physics
in partial fulfillment of the requirements for the degree of

Bachelor of Science in Physics

at the

MASSACHUSETTS INSTITUTE OF TECHNOLOGY

June 2014

Author . . . .
Department of Physics
May 8, 2014

Certified by. . . . .
Wolfgang Ketterle
Professor
Thesis Supervisor

Accepted by . . . .
Nergis Mavalvala
Senior Thesis Coordinator, Department of Physics

Realization of Bose-Einstein Condensation with Lithium-7 Atoms

by

Yichao Yu

Submitted to the Department of Physics
on May 8, 2014, in partial fulfillment of the
requirements for the degree of
Bachelor of Science in Physics

Abstract

This thesis presents our work on developing and improving the techniques of trapping and cooling an ultra-cold cloud of Lithium-7 atoms and the realization of the Bose-Einstein condensate as a first step to study quantum magnetism in optical lattice. The techniques used in this experiment includes Zeeman slower, magneto-optical trap (MOT), gray molasses, static magnetic trap, evaporative cooling, optical dipole trap (ODT), etc. The apparatus has the capability of creating a Bose-Einstein condensate with almost 10^6 atoms in 10 seconds as well as tuning the interaction between atom in a BEC using the Feshbach resonance with a magnetic bias field up to $\approx 1000G$.

Thesis Supervisor: Wolfgang Ketterle
Title: Professor

Acknowledgments

First I would like to thank Professor Wolfgang Ketterle for giving me the chance to work in his new Lithium-7 group. I have really learned a lot from working on the experiment and his special vision about the field of ultracold atoms.

I would also like to thank the three senior graduate students working in this laboratory, Jesse Amato-Grill, Ivana Dimitrova and Paul Niklas Jepson for setting the experiment up from scratch and pushing it forward, and our new graduate student William David Lunden for writing and maintaining a nice data acquisition system, among other things. Special thanks also to the member of my previous laboratory, Hiro Miyake, Georgios Siviloglou, David Weld and Colin Kennedy for leading me into the field and teaching me many useful skills.

Finally, I am specially grateful for my parents, my cousin, my uncle, my aunts and my grandparents for understanding and supporting me during my undergraduate study at the Massachusetts Institute of Technology.

Contents

List of Figures

List of Tables

Introduction

Predicted in 1924-25 by Satyendra Nath Bose and Albert Einstein from Bose statistics, the Bose Einstein condensate is a phase of matter at ultra-cold temperature that emerges completely because of quantum effect. It was first produced in the laboratory in 1995-96 at the University of Colorado Boulder, Massachusetts Institute of Technology and Rice University using laser cooling and evaporative cooling techniques. Since then, people have been using it to study many quantum effects. Among them, one effort is to simulate complex condensed matter systems using simplfied and well controlled model systems created by loading BEC into optical lattices.

In our experiment, we use the Lithium-7 atoms to create Bose-Einstein condensate. Because of the lightness and several Feshbach resonances, the Lithium-7 atom has very fast dynamics and great tunability, making it a perfect candidate for simulating and studying the phase diagrams of certain condensed matter models. The ultimate goal of the experiment is to study the anti-ferromagnetic phase in the anisotropic Heisenberg model (XXZ model) and the work in this thesis focuses on getting a Bose-Einstein condensate using Lithium-7, one of the important steps before studying the system in an optical lattice.

The presentation of this thesis is divided into two chapters. In the first chapter, I discuss the theory of our experiment, including the Bose-Einstein condensate (BEC) and the various cooling and trapping techniques we use. The second chapter describes the setup of the experiment, the alignment and optimization procedure we developed and the experimental result we have got for each steps.

Chapter 1

Theory

In this chapter, I am going to describe the theories behind our experiment. It is divided into three parts. The first section explains the theories of cold Bose gas and the Bose-Einstein condensation relevant to the experiment. The second section briefly describes some important properties of the Lithium-7 atom. Finally, in the third section, the cooling, trapping and state manipulation techniques used in the experiment are presented, including Zeeman slower (1.3.1), MOT(1.3.2), gray molasses (1.3.3), magnetic trap (1.3.4) and optical dipole trap (1.3.5).

1.1   Bose-Einstein Condensate in Harmonic Trap

Every real particles can be classified as one of the two families according to their spins, fermions which have half integer spins and bosons which have integer spins. According to quantum field theory[1, 4] the many-particles wave function of identical particles must be symmetric or anti-symmetric under particle exchange for bosons or fermions respectively. For bosonic particles, because of the symmetry of the wave function, the possibility for particles to be in the same state is greatly enhanced. As a result, boson gas at ultra-low temperature forms a Bose-Einstein condensate (BEC), in which almost all of the particles are condensed to the lowest energy state. In the following, the relevant properties of BECs such as critical temperature and density distribution are described.

Since the wave function of bosons is symmetric, multiple bosons can be in the same state. From this fact, the energy distribution can be calculated for bosons,

$$f(\varepsilon) = \frac{1}{e^{\beta(\varepsilon-\mu)} - 1}$$

Since the distribution has to be positive for all energy states, in particular the $\varepsilon = 0$ ground state, we have $\mu \geqslant 0$. For all the state except the ground state, this sets an finite upper limit on the number of atoms in each state for a fixed temperature. Therefore, if the number of atoms exceeds a certain value, all the extra atoms will go into the ground state. These atoms condensed in the ground state are called the Bose Einstein condensate.

In order to calculate the atom number in the condensate as well as the critical temperature, we can estimate the maximum atom number in the excited states (thermal atoms) with an integral,

$$N_{th} = \int_0^\infty \frac{g(\varepsilon)}{e^{\beta\varepsilon} - 1} d\varepsilon$$

where $g(\varepsilon)$ is the energy density of states. In our experiment, we create the BEC in a harmonic optical dipole trap (see 1.3.5) for which the density of states is,

$$g(\varepsilon) = \frac{\varepsilon^2}{2\hbar^3\omega^3}$$
$$N_{th} = \frac{1}{2\hbar^3\omega^3} \int_0^\infty \frac{\varepsilon^2}{e^{\beta\varepsilon} - 1} d\varepsilon$$
$$= \frac{1}{2\hbar^3\omega^3\beta^3} \int_0^\infty \frac{x^2}{e^x - 1} dx$$
$$= \frac{k_B^3 T^3}{2\hbar^3\omega^3} \zeta(3)\Gamma(3)$$

The critical temperature of the transition, determined by $N_{th} = N$,

$$T_C = \frac{\hbar\omega}{k_B}\sqrt[3]{\frac{2N}{\zeta(3)\Gamma(3)}}$$
$$= 0.9405\frac{\hbar\omega\sqrt[3]{N}}{k_B}$$

Condensate fraction (for large N),

$$\frac{N_0}{N} = 1 - \frac{N_{th}}{N}$$
$$= 1 - \left(\frac{T}{T}\right)^3$$

1.2   Lithium-7 Atoms

The atoms used in this experiment is the Bosonic isotope of Lithium, Lithium-7. In this section, I will present some properties of the Lithium-7 atoms that are important for the cooling and trapping techniques we use in the experiment.

One of the most important properties for laser manipulation of cold atoms is the energy level structure. As all other alkali atoms, Lithium-7 has one unpaired valence electron with a nS ground state and nP excited states, where $n = 2$ for Lithium-7. The fine structure split the excited states into $2^2P_{1/2}$ and $2^2P_{3/2}$ states corresponding to the $D1$ and $D2$ lines that are about $10GHz$ apart. On top of these, the hyperfine structure caused by the nucleus spin ($I = 3/2$ for Lithium-7) further split each of these states into different levels with different total angular momentum F. the precise frequencies of these transitions measured in the experiment are shown in figure 1-1

In an external magnetic field, each $F \neq 0$ levels will be split because of the Zeeman effect. At low field, this splitting is described by the Landé g-factor $\Delta = g_F\mu_B m_F B_z$ as shown in table 1.1. At higher magnetic field, different hyperfine levels starts to

$F = 0$

2.759(27)MHz

$F = 1$

5.813(27)MHz

$F = 2$ $2^2 P_{3/2}$

9.462(27)MHz

$F = 3$

$F = 2$

91.877(9)MHz $2^2 P_{1/2}$

$F = 1$

D1
446.799 862 994(12)THz
(670.977 058 925(18)nm)

D2
446.809 874 988(27)THz
(670.962 023 854(41)nm)

$F = 2$

803.504 086 6(10)MHz $2^2 S_{1/2}$

$F = 1$

Figure 1-1: Energy level structure of Lithium-7[5]

Table 1.1: Landé g-factors of Lithium-7

Fine Structure	F	g-factor
$2^2S_{1/2}$	2	$\dfrac{1}{2}$
	1	$-\dfrac{1}{2}$
$2^2P_{1/2}$	2	$\dfrac{1}{6}$
	1	$-\dfrac{1}{6}$
$2^2P_{3/2}$	1, 2, 3	$\dfrac{2}{3}$

mix and the Zeeman effect is no-longer linear. Most importantly, for $2^2S_{1/2}$ ground states the $F = 1$ states have a negative slope at high magnetic field and all the $F = 2$ states except $m_F = -2$ has a positive slope. (Note that F and m_F are no-longer good quantum numbers at high magnetic field but there are states at high field that are adiabatically connected with these F and m_F eigenstates). The states with a positive slope of the Zeeman shift are magnetically trappable states since they can be trapped by a static magnetic field which can have a local minimum (but not a maximum [1.3.4]) in the center. The $m_F > 0$ states are trappable at low field and all the $F = 2$ states are trappable at high field. In particular, only $|F = 2, m_F = 2\rangle$ and $|F = 2, m_F = 1\rangle$ states are both trappable at high field and low field. This is important for our experiment because we would like to use a stronger magnetic confinement to compress the could in order to get higher density and higher collision rate.

1.3   Cooling and Trapping Theory

The atoms used in an alkali atom experiment often come from an atom beam coming out of a oven kept above the melting temperature of the metal. The oven used in this experiment operates at 485°C producing an atom beam traveling at several hundred meters per second. In order to achieve low temperature and high density, several stages of slowing, trapping and cooling are implemented in this experiment

which finally bring the atoms down to the Bose-Einstein condensate condition. In this section, I am going to talk about the theory behind these techniques we are using in our experiment.

1.3.1 Zeeman Slower

The atoms comes out of the oven has an average velocity determined by the Maxwell-Boltzmann distribution,

$$\bar{v} = \sqrt{\frac{k_B T}{2\pi m}}$$

We can slow down the atoms using the recoil of photon scattering by shining resonance light onto the atomic beam. However, since the atomic transition resonance is very narrow ($\Gamma = 2\pi \cdot 5.9\text{MHz}$) compare to the Doppler shift ($\Delta\nu = \nu v/c \approx 590\text{MHz}$), the atom will soon shift out of resonance once it slows down. There are several ways to solve this problem. One way is to modulate the laser frequency, either sweeping with time (frequency chirping) or making it broadband (white light). The Zeeman slower solves the problem by changing the resonance of the atom with the Zeeman effect. This is the most popular way for alkali atoms which all have a cycling transition with a linear Zeeman effect in a large range of magnetic fields[6].

The Zeeman slower has a magnetic field aligned with the atom beam with a spatially varying amplitude. By shining circularly polarized light against the atom beam, the atoms in the beam are optically pumped to one of the two stretched states determined by the relative direction of the field and the light polarization. If the magnetic field is changing in a way such that the Zeeman shift of the atom follows the Doppler shift when atoms slow down, the atom beam will be always in resonance and continuously being slowed down, i.e.

$$g_F m_F \mu_B B = \frac{v}{c}\nu + \Delta$$

For constant acceleration, this implies,

$$B = \frac{\sqrt{v_0^2 - 2ax}}{g_F m_F \mu_B c} \nu + B_0$$

The maximum deceleration of the Zeeman slower is limited by the maximum scattering rate, therefore the life time of the excited state,

$$a_{max} = \frac{h\Gamma}{2\lambda}$$

where Γ is the linewidth of the transition.

1.3.2   Magneto-Optical Trap (MOT)

As in most cold atom experiment, our experiment starts with loading Zeeman slowed atom into a magneto-optical trap (MOT). MOT is a technique that uses laser and magnetic field gradient to provides both molasses cooling and confinement[6]. In order to understand how the MOT works, we will consider a one-dimensional model consisting of a spatially varying magnetic field $B = B_x = B'x$, two counter propagating, red-detuned, circularly polarized light with atoms sitting close to the zero of the magnetic field.

The cooling and trapping effect in a MOT can be understood separately. Let us first consider an atom in the center of the MOT moving in the $+x$ direction. Since the light is red-detuned, the Doppler effect will shift the atom closer to the light in $-x$ direction and farther from the light in $+x$ direction. The atom will therefore scatters more photons from the $-x$ light and experience an average force proportional but in the opposite direction with its velocity. Such a force will damp the motion of the atom and therefore cool down the temperature of the cloud.

In order to understand the source of the trapping force in a MOT, we can consider an atom with a $F = 0$ ground state and $F = 1$ excited states. As we can see in the
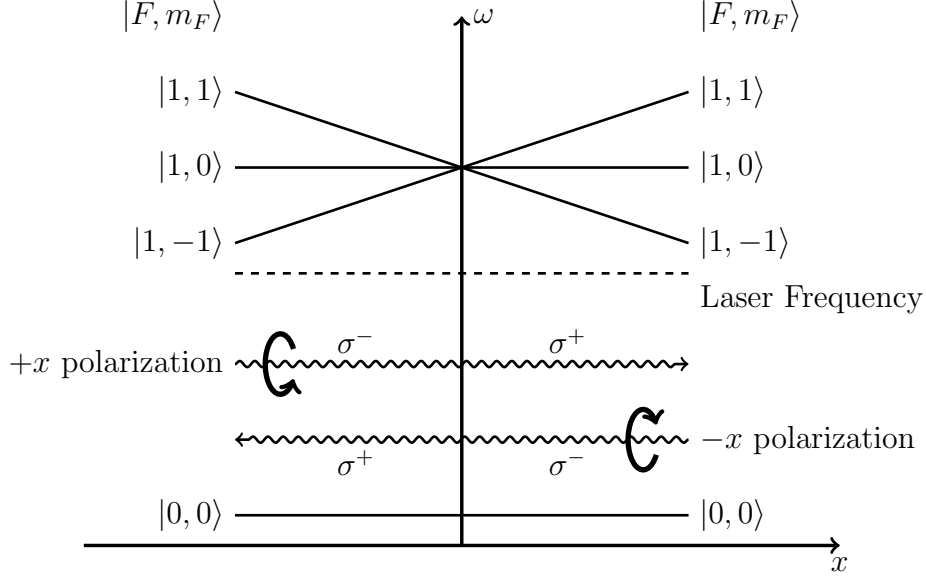
Figure 1-2: Schematic of a $1D$ MOT with a $F = 0$ to $F = 1$ transition.

schematic of this model (Figure 1-2), since the magnetic field changes its direction in the center, both laser beams are σ^- light on the side it is coming from and therefore is shifted closer to resonance by the Zeeman effect. Therefore, atoms shifted from the center will scatter more photon from this direction and on average feel a net force from recoil pointing toward the center of the trap.

According to the above discussion, the force an atom feels in the MOT comes from the difference in the scattering rate from the pairs of counter-propagating beams, which can be expressed as,

$$
\begin{aligned}
F =& \hbar k \left(w\left(\delta_0 + \frac{\omega}{c} v + \frac{g\mu_B B'}{\hbar} x \right) - w\left(\delta_0 - \frac{v}{c}\omega - \frac{g\mu_B B'}{\hbar} x \right) \right) \\
\approx& 2\hbar k \left. \frac{\mathrm{d}w}{\mathrm{d}\delta} \right|_{\delta=\delta_0} \left(\frac{\omega}{c} v + \frac{g\mu_B B'}{\hbar} x \right) \\
=& -2\hbar k \left| \frac{\mathrm{d}w}{\mathrm{d}\delta} \right|_{\delta=\delta_0} \left| \frac{\omega}{c} v - 2g\mu_B B'k \left| \frac{\mathrm{d}w}{\mathrm{d}\delta} \right|_{\delta=\delta_0} \right| x
\end{aligned}
$$

where $\hbar k$ is the recoil momentum of a single photon, $w(\delta)$ is the scattering rate as a function of the detuning, δ_0 is the laser detuning, $\frac{\omega}{c} v$ is the doppler shift, and

$\dfrac{g\mu_B B'}{\hbar}x$ is the spacially varying Zeeman shift. As we can see, both the cooling and confining force are proportional to the derivative of the scattering rate and therefore is generally larger with smaller detuning (until $\Gamma/2$). However, since the heating from photon scattering is also larger at smaller detuning, this limits the lowest possible temperature achievable by the MOT (Doppler limit). The temperature and atom density in the MOT is also limited by the rescattering of light and light induced collisions.

1.3.3 Gray Molasses

The $2^2P_{3/2}$ excited state of Lithium-7 we use for molasses cooling in the MOT does not have resolved hyperfine structure (Figure 1-1). Therefore, we cannot form conventional polarization gradient cooling using the $D2$ line. Instead, we implement a gray molasses on the D1 transition. This scheme was first studied and demonstrated by Christophe Salomon[2] to achieve sub-Doppler temperature on some alkali isotopes that are not amenable for conventional polarization gradient cooling (^7Li, ^6Li and ^{40}K). In this section, I am going to present a semi-quantitative explanation of this cooling scheme. See the original paper[2] for more detail discussion.

The gray molasses cooling uses three pairs of counter-propagating beams that can cool the cloud in all three dimensions. Like what we did for MOT, we will consider a $1-D$ case for simplicity. The model we will use has a pair of counter-propagating beams, each has a high intensity pumper, with a large blue detuning δ from the $F=2$ ($|2\rangle$) to $F'=2$ ($|3\rangle$) D1 transition, and a low intensity repumper, blue detuned from the $F=1$ ($|1\rangle$) to $F'=2$ D1 transition by the same detuning δ. Let the Rabi frequency for the pumper and the repumper be $\Omega_2(x)$ and $\Omega_1(x)$ respectively.

Just as any other laser cooling method, the performance of the gray molasses is determined by the balance between cooling force and heating from photon scattering. Since the two beams (pumper and repumper) satisfies the Raman resonance
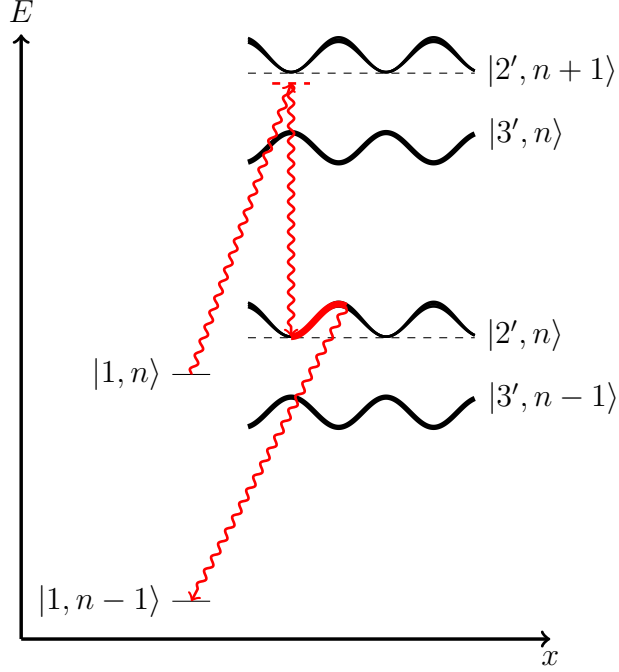
Figure 1-3: Schematic of a $1D$ Gray Molasses.[2]

condition, the system has a dark state which is a superposition of $|1\rangle$ and $|2\rangle$,

$$|NC\rangle = \frac{\Omega_2|1\rangle - \Omega_1|2\rangle}{\sqrt{\Omega_1^2 + \Omega_2^2}}$$

which will be the state most of the atoms will be pumped into. (The state is dark for stationary atoms and has a non-zero but small scattering rate for moving atoms.) Since the scattering is suppressed by the present of a dark state, the gray molasses produce little heating.

The cooling effect of the gray molasses can be understood in the dressed atom picture for the atom and the pumper beam as shown in figure 1-3, where the new energy eigenstates are,

$$|2'\rangle = \frac{\delta^2}{\delta^2 + \Omega_2(x)^2}(|2\rangle - i\Omega_2(x)|3\rangle)$$
$$|3'\rangle = \frac{\delta^2}{\delta^2 + \Omega_2(x)^2}(|3\rangle - i\Omega_2(x)|2\rangle)$$

24

Since the detuning δ is large, the mixing between $|2\rangle$ and $|3\rangle$ is small giving $|3'\rangle$ a short lifetime and $|2'\rangle$ a longer lifetime. The two counter-propagating pumper beams create a standing wave which causes periodic AC-Stark shift in the dressed $|2'\rangle$ and $|3'\rangle$ states. A repumper with the same or slightly smaller blue detuning compared to the pumper is closest to the resonance with the dressed states at the nodes of the standing wave where the mixing is minimized. Therefore, the repumper most likely pumps atoms into the $|2'\rangle$ state (through $|3'\rangle$ as shown in figure 1-3) at the node of the standing wave and the atoms will most likely exit the state at the anti-node of the standing wave where the lifetime of $|2'\rangle$ is the shortest because of the maximum mixing. Since potential energy for atoms in $|2'\rangle$ is minimized at the nodes and maximized at the anti-nodes, this is a realization of the Sisyphus cooling scheme in which the atoms feel on average a damping force by climbing up the hill repeatedly in $|2'\rangle$. The height of the hill, therefore the cooling force, is proportional to the laser intensity. Combined with the low scattering rate due to the dark state, the gray molasses can be used to quickly cool the cloud after MOT to sub-Doppler temperature.

1.3.4   Evaporation in a Static Magnetic Trap

The density and temperature of a laser cooled cloud is usually limited by the scattering of photons. Therefore, in order to reach quantum degeneracy, one usually needs to use a way that can cool the atoms without shining resonant light onto them. The method we use in our experiment is evaporative cooling in a magnetic trap and an optical dipole trap. In this section, I will describe the theory of static magnetic quadrupole trap and radio frequency evaporation and the theory of evaporation in an optical dipole trap will be discussed in the next section.

The static magnetic trap, as the name suggested, is created using static magnetic field and the Zeeman effect of the atoms. Assuming a monotonic the Zeeman effect, the atoms will be trapped at an extremum of the field. Since the magnetic field in

the vacuum satisfies the source-less Maxwell equation, we have,

$$
\begin{aligned}
0 =& \nabla \times (\nabla \times B) \\
=& \nabla(\nabla \cdot B) - \nabla^2 B \\
=& -\nabla^2 B \\
\nabla^2(B^2) =& 2\nabla(B \cdot \nabla B) \\
=& 2(\nabla B)^2 + 2B \cdot \nabla^2 B \\
=& 2(\nabla B)^2 \\
\geqslant& 0
\end{aligned}
$$

Therefore, the only local extremum that is possible for a static magnetic field in the vacuum is a local minimum and only states with a positive Zeeman shift (low field seeking) can be trapped magnetically (known as Wing's theorem[7]).

The static magnetic field with a local minimum in the center can be implemented in many different ways. The configuration used in this experiment is a quadrupole field created by a set of Helmholtz coils carrying opposite current, which provides tighter confinement compared to other configurations. Closed to the center of the trap, the magnetic field can be expressed as,

$$
\begin{aligned}
B_x =& B'x \\
B_y =& B'y \\
B_z =& -2B'z
\end{aligned}
$$

Since the magnetic field is 0 at the center of the trap where all the Zeeman levels are degenerate, spin-flips of atoms (Majorana loss) occurs in the center of a quadrupole trap. This problem is fixed in the experiment by plugging the hole with a repulsive blue detuned laser beam. This problem as well as the solution will be further discussed in the experimental chapter (2.6)

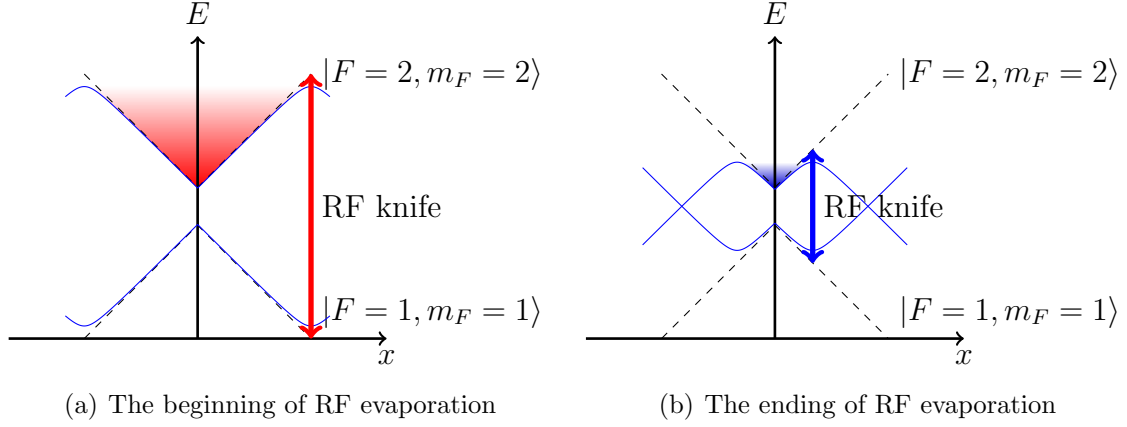(a) The beginning of RF evaporation   (b) The ending of RF evaporation

Figure 1-4: RF evaporation in magnetic trap. The temperature goes down and the phase space density goes up during evaporation.

After trapping the atoms with the magnetic field, we use radio frequency induced spin-flip to evaporate the cloud. As shown in figure 1-4, the $|F = 2, m_F = 2\rangle$ has a positive slope of the Zeeman shift whereas the $|F = 1, m_F = 1\rangle$ state has a negative one. After all the atoms are trapped in the $|F = 2, m_F = 2\rangle$ state, a RF field that is blue detuned to the zero field resonance is applied which mixes the two states and turns the potential curve around at the resonance field. As a result, the depth of the trap is lowered and atoms which has higher energy can now escape from the trap. If the RF knife is placed much higher than the thermal energy $k_B T$, each leaving atoms will carry away energy a lot higher than the average value leaving a lower average energy, therefore lower temperature, for the atoms remaining in the trap. After the cloud gets colder, fewer and fewer atoms will have the energy to pass the RF knife, at which point the RF frequency can be sweep down to accelerate the evaporation. In order for the evaporative cooling to work efficiently, a high elastic collision rate (high rate for creating atoms with high energy) is also necessary.

1.3.5 Evaporation in Optical Dipole Trap

Although RF evaporation in the magnetic trap is very convenient and efficient, it does have some limitations,

1. The atoms have to be in a specific hyperfine state.

2. Cannot use a Feshbach resonance to tune the interaction with magnetic field.

Moreover, for Lithium-7, the trappable $|F = 2, m_F = 2\rangle$ state has a negative scattering length $(-27a_0)$ making it impossible to create a stable Bose-Einstein condensate with a large atom number. In order to solve the problem, we switch to an optical dipole trap and do the final evaporation there.

The optical dipole trap (ODT) is created using the negative AC Stark shift of a red detuned laser beam. Since the AC Stark effect is proportional to δ^{-1} (where δ is the detuning) and the scattering (heating) is proportional to δ^{-2}, high power beams with huge detuning $(\approx 100THz)$ are often used in order to introduce the least amount of heating for the same trapping potential.

Evaporation in an ODT is done simply by lowering the potential (beam power). Since a positive and big scattering length is necessary for efficient evaporation to BEC, we spin-flip the atoms into $|F = 1, m_F = 1\rangle$ and evaporate close to a Feshbach resonance with an appropriate scattering length.

Chapter 2

Experimental Setup and Results

In this chapter, I will describe our experimental setup and results. It includes a brief discussion of our optical tables setup (2.1 and 2.2), the implementation, optimization and performance of each steps (2.3, 2.4, 2.5, 2.6 and 2.7) and finally some basic characteristic of our BEC (2.7). The discussion will fucus mainly on the main coil configuration (2.2.3), gray molasses alignment (2.4) and stray field zeroing for the quadrupole magnetic trap 2.6 in which I had the most contribution.

The other important parts of the experiment are going to be discussed briefly in order to give a complete picture of the experiment. A more detailed description of some part of the experiment, especially the vacuum system, the laser system, the optimization of the RF evapration in the magnetic trap, the optical dipole trap and the BEC, are expected to be found in the PhD thesis of the current senior graduate students.

2.1   Laser System

The laser table is where we prepare all the light sources used in the experiment that is closed to resonance with the Lithium-7 $D1$ and $D2$ lines. In this section, I will give a description of our laser system. Instead of going into technical details about the setup, which will be included in one of the future PhD thesis, I am going to briefly

describe the goal of the system, the techniques we use, and the performance of it.

As discussed in the theoretical chapter, we need mainly four different frequency ranges for the laser cooling and manipulation of the atoms. For the Zeeman slower and MOT, we need the $D2$ line (1.3.2) and we use the $D1$ line for the gray molasses (1.3.3). For the dark state pumping that will be discussed later (2.5), we also use the $D1$ line. Furthermore, in all of these cases, we also need two frequencies to address the atoms in both of the hyperfine ground states $F = 1$ and $F = 2$, which are conveniently called $F1$ and $F2$ light. The goal of the laser table is therefore generating these four different frequencies ranges and deliver them to the machine table using optical fibers.

Since the separation between $D1$ and $D2$ is larger than most of the common optical frequency shifters (e.g. AOMs), we generate the $D1$ and $D2$ light by locking two diode lasers on to the appropriate atomic transition using saturated absorption spectroscopy. Since we do not need $D1$ and $D2$ light at the same time, we use an AOM in each of the $D1$ and $D2$ beam path to swich the light and determine which frequency goes to the rest of the system. In the $D2$ path, we also use a $300MHz$ AOM in the double pass setup to get the right frequency for the Zeeman slower.

After selecting one of the D lines, we use a 50-50 cube beam splitter to put them into the $F1$ and $F2$ path. Since the hyperfine splitting of the ground state for Lithium-7 is relatively small ($803.5MHz$), we use a $400MHz$ AOM in the double pass setup to blue shift the frequency from $F2$ to $F1$ and to fine tune the frequency in certain range. For the $F2$ pass, two AOM's in the tandem setup are used for frequency fine tuning.

The frequency generation stage is followed by an amplification stage using one tapered amplifier per-path to generate the power we want. After that we use AOM's, shutters and other optics to switch the laser, couple them into the fibers with the right polarization and deliver them to the machine table where we use them to manipulate

Figure 2-1: Top View of the Vacuum Chamber (Top/Bottom MOT/Gray Molasses (GM) beams not included, not to scale).

the atoms.

2.2 Vacuum Chamber and Main Coils Configuration

In this section, I am going to describe some important feature of the setup on the machine table where the vacuum chamber is mounted.

2.2.1 Optical Access of the Vacuum Chamber

The windows and connections except the top and bottom window on our main vacuum chamber is shown in figure 2-1. There are in total 6 MOT/Gray Molasses beams, 2 ODT beams, 3 Imaging beams, a plug and a Zeeman slower beam going into the chamber. When multiple colors need to be sent in through the same window, they are combined outside the vacuum chamber using appropriate dichroic mirrors.

Figure 2-2: MOT/Gray Molasses Cage. $\updownarrow$'s represent lenses.

2.2.2 MOT-Gray Molasses Cage

The delivery of the MOT and gray molasses beam from the laser table to the machine table is done with a polarization maintaining evanescent wave fiber splitter which takes the light from the two input fibers and split them equally into six output fibers. However, the MOT beams and the gray molasses beams have different requirements in beam sizes. On one hand, the MOT needs a bigger beam size for a bigger capture volume. On the other hand, as discussed earlier, for the gray molasses to work effectively, high intensity, therefore smaller beam size, is required. In order to have a different size for the two beams coming out of the same fiber, we send in the two beams with orthogonal polarizations and add polarization dependent beam expenders after the fiber output to shape the two beams differently. This beam shaping is done with a cage system shown in figure 2-2. The upper beam path is used for expanding the MOT beam whereas the lower path shapes the gray molasses beam to a smaller size. Each of the four lenses can slide in the cage, which are used to tweak the size and divergence of the beams. The alignment between beams is done with the two bottom mirrors and the two half wave-plates between the two polarization beam splitter cubes are used to balance the intensities.
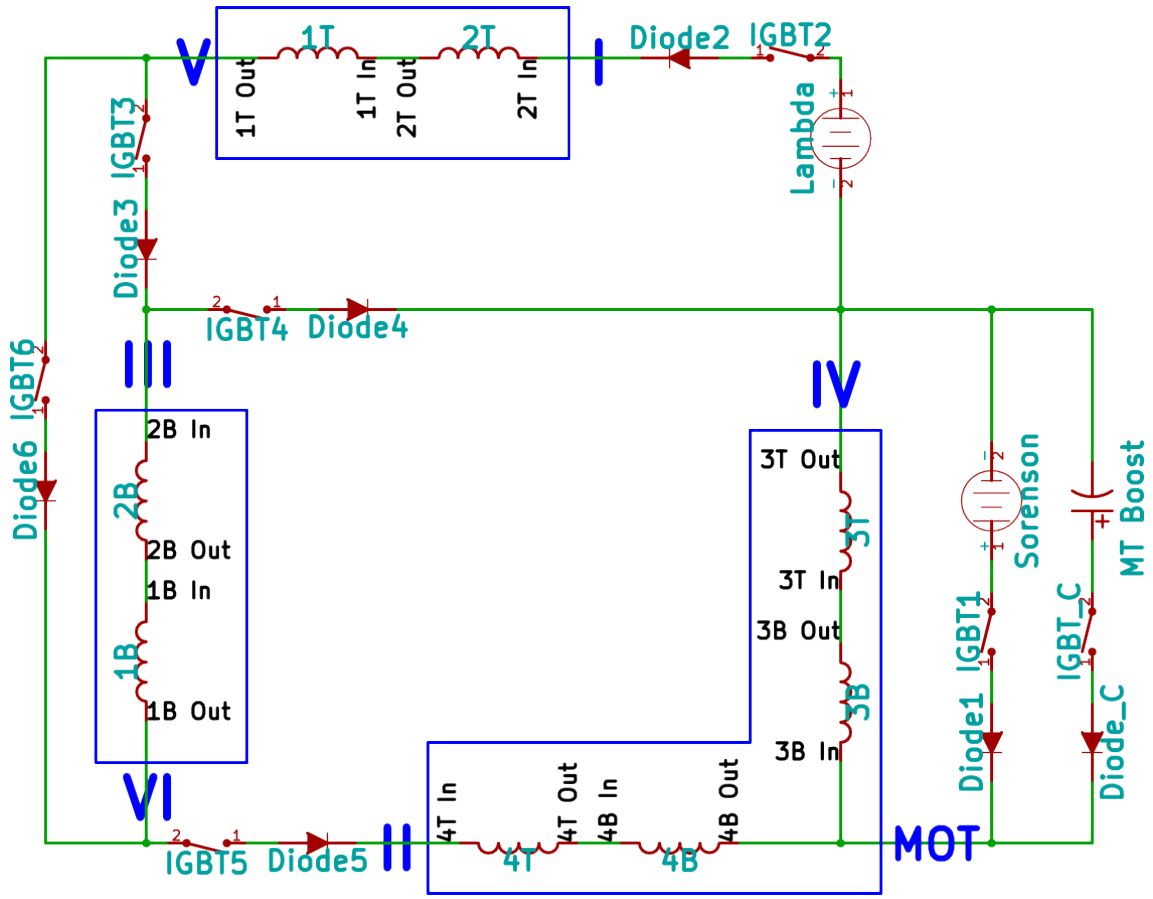
Figure 2-3: Main Coils Control Circuit. (Magnetic trap boost capacitor charging circuit not included.)

Closed switches(IGBTs)	Usage of the power supply	
	Lambda	Sorenson
1, 3, 5	-	Quadrupole field with layer 3 for MOT and ODT clean up (2.7)
2, 3, 5	Quadrupole field with layer 1, 2, 3 and 4 for magnetic trap	-
1, 2, 4, 6	Homogeneous Feshbach resonance field with layer 1 and 2	Field gradient on top of the bias field with layer 3 for tilt and levitation.

Table 2.1: List of coil configurations

2.2.3   Main Coils Configuration

Besides the weak field (up to several Gauss) provided by the shim coils for earth field compensation and small bias fields, we use strong magnetic fields in the experiment in many different configurations. In the magneto-optical trap, we need a quadrupole field ($\approx 20\mathrm{G}\cdot\mathrm{cm}^{-1}$). For the static magnetic trap, we use a stronger quadrupole field ($\approx 500\mathrm{G}\cdot\mathrm{cm}^{-1}$). And finally for the evaporation in the optical dipole trap, we need independent control of a very strong bias field (up to $\approx 1000\mathrm{G}$) and a gradient on top of it (up to $\approx 30\mathrm{G}\cdot\mathrm{cm}^{-1}$). Moreover, in order to avoid loss of atom number and density between steps with different field requirements, we also need the capability of turning on and off or changing the configuration of the magnetic field quickly ($\ll 1\mathrm{ms}$).

These strong magnetic field is generated in the experiment by running up to 500A of current through one pair of water cooled coils attached to the vacuum chamber. The coils are positioned closed to the Helmholtz condition to maximize the homogeneity when generating a bias field. Each of the coil consists of 5 layers which can be connected and powered independently (one of them got damaged during operation and is not currently used) so that they can be used in different configurations. Due to the limitation of our power supplies (both in output capability and in the number we have), many of the field configuration we need requires running current through more than one layer of the coils. Therefore, in order to achieve different configuration of the field, it is necessary to reuse our power supplies and coil layers in different steps.

The options available for fast switching of such high current are mechanical relays or solid state (semiconductor) devices. After comparing the performance and reliability of different options, we decided to use high power IGBT's (insulated-gate bipolar transistor) since they are the most widely used solid state device for high current application and can provide much shorter response time with similar cost and failing rate compared to mechanical relays. The switching time for these IGBT's to switch certain current are determined by the response time of the device (micro-seconds or

shorter) and the maximum voltage they can take (since $\mathrm{d}I/\mathrm{d}t = L/U$). Since the IGBT's we use can take a voltage higher than 500V, simple calculation shows that they can switch off the maximum current we have within $100\mu s$, which is already much shorter than the decay time of the eddy current in our vacuum chamber (milli-second).

In order to generate bias fields and quadrupole fields with our main coil unit, we can put current into one pair of layers on both sides in the same and opposite direction respectively. However, for reusing a layer, we need to switch the polarity of current on one side and keep the direction on the other side the same. Since each IGBT acts like a single throw single pole switch (in one direction), we need four IGBT's (two on each side) to change the polarity of one layer by connecting the two ends of the layer to either side of the supply. This configuration is called a H-bridge. In addition to this, since each of the four switches are closed only in one case, we can put layers in series with one of the switches so that they are only powered in one of the configurations in order to use different number of layers in the two configurations. After considering other factors including geometrical constraint and convenience the modified H-bridge designed we use in our experiment can be seen in figure 2-3. "Lambda" and "Sorenson" are the two power supplies. Each pair of switch and diode represent an IGBT module with floating TTL input control. The layers are numbered from $1-4$ starting with the inner most layer (closest to the atoms). T and B denote the top and bottom part of the coil unit. The "in" and "out" labels on the layer terminal represent the direction of the current to generate a quadrupole field. Finally, the blue lines separate the parts on the machine table (coils) and the parts on the power supply rack (power supplies and IGBT's) and the blue labels are the connections between the two places. This plot also shows the capacitor (MT Boost) used to boost the magnetic trap turn on with a high voltage. The summary of possible configurations are shown in table 2.1.
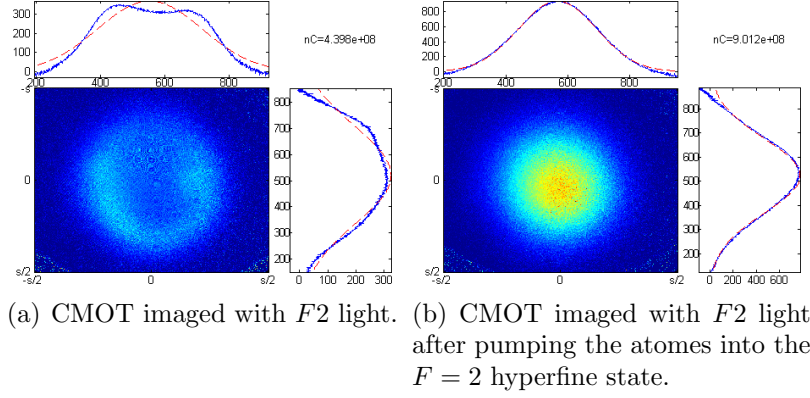
(a) CMOT imaged with $F2$ light. (b) CMOT imaged with $F2$ light after pumping the atomes into the $F = 2$ hyperfine state.

Figure 2-4: Image of the CMOT. Atoms are pumped into the $F1$ states.

MOT power	Repumper power	MOT detuning	Repumper detuning	MOT Current
16mW	7mW	-38.5MHz	-28MHz	57A

Table 2.2: MOT parameters

2.3 Magneto-Optical Trap (MOT) and Compressed-MOT

As the first step of the laser cooling, the MOT loading is optimized by changing the parameters of the lasers to maximize the number of atoms in the MOT after 6 seconds of loading. The optimum settings we have found are listed in table 2.2 and the performance of our MOT can be found in table 2.3.

Since our MOT is mainly optimized for loading rate, it is not necessarily optimized for high density and low temperature. Therefore, we added a compressed-MOT (CMOT) step after the MOT in order to increase the density and decrease the temperature. In the CMOT step, we ramp the MOT frequency closer to resonance in 4.5ms and decrease the intensity of the repumper. As a result, the cloud is compressed by radiation pressure and pumped to the $F = 1$ state. The temperature of the cloud is also decreased because of the decrease in scattering. Figure 2-4 shows that the atoms in the CMOT are pumped into the $F = 1$ states and the performance of the CMOT
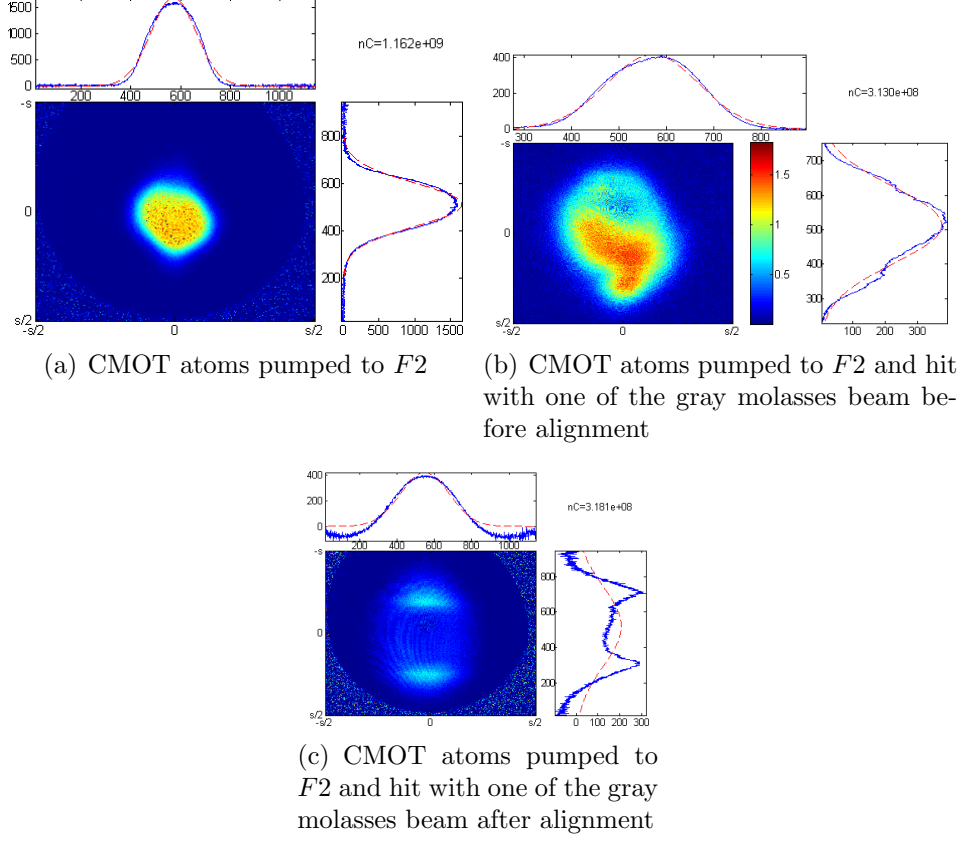
(a) CMOT atoms pumped to $F2$

(b) CMOT atoms pumped to $F2$ and hit with one of the gray molasses beam before alignment

(c) CMOT atoms pumped to $F2$ and hit with one of the gray molasses beam after alignment

Figure 2-5: Images used to align the gray molasses beams.

is listed in table 2.3.

2.4 Gray Molasses

The gray molasses step is used to cool the CMOT cloud further before transferring the atoms to the magnetic trap for evaporative cooling. As mentioned before, we use a smaller size for the gray molasses beam for higher density and better cooling performance. Since the gray molasses only works when the atoms are hit by all of the three pairs of counter-propagating beams, with a gray molasses beam size comparable to that of the cloud after CMOT (both have diameter $\approx$ 5mm), one of the challenging tasks for optimizing the gray molasses is to maximize the overlap between the cloud and the six beams while making sure each pairs of the beams are well aligned.
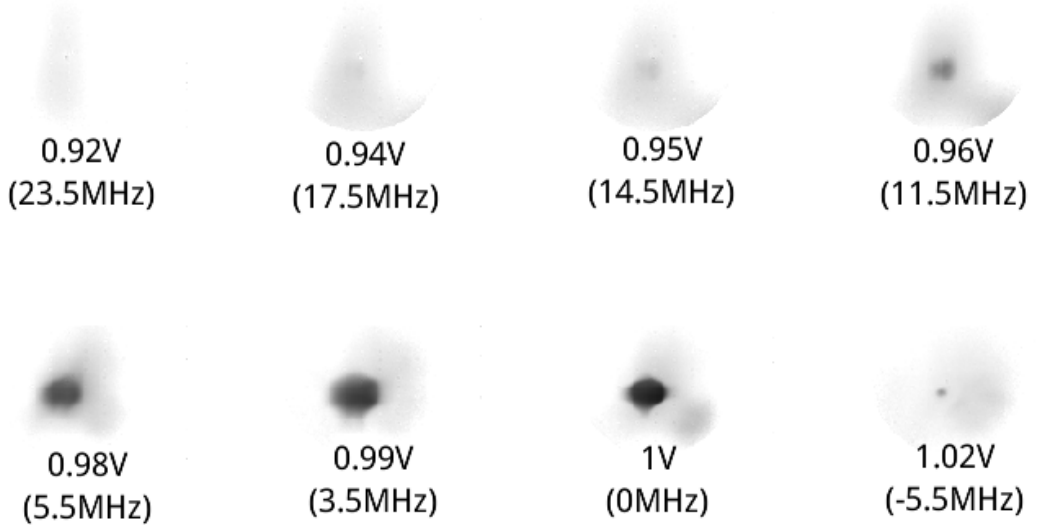
Figure 2-6: Time of flight image for gray molasses with different relative detuning (in MHz) between the pumper and repumper. (The voltages in the image is the control voltage we use to adjust the frequency.)

Several strategies have been tried to align the gray molasses beams to the desired precision including overlaping with the MOT beams in the far field, centering on the window of the vacuum chamber etc. However, since most of these methods relies on the geometry of the machine rather than the atom, we were not able to get the performance we want.

In order to overcome this problem, I came up with a method to directly align the beams with the cloud after CMOT to high precision, which can achieve good alignment reliably. The idea is to image the part of the cloud that is missed by each of the beams and to use this image to center the beam on the cloud and minimizing the missing atoms number. In the experiment, this is done by first optically pumping all the CMOT atoms into $F = 2$ state (figure 2-5(a)) and then illuminate the cloud with a short pulse of $F = 2$ light from one of the gray molasses beam path while blocking other beams (this is possible without affecting the previous steps because the MOT and gray molasses beams use different beam paths). Although the atoms hit by the beam will not move far because of the recoil, the short pulse is enough to pump them into the $F = 1$ state. Therefore, imaging with $F = 2$ light without a $F = 1$ repumper

Step	Atom Number	Temperature(K)	Density(cm^{-3})
Oven	-	760	-
Zeeman Slower	-	0.5	-
MOT	$2 \cdot 10^{10}$	$1.5 \cdot 10^{-3}$	$1 \cdot 10^{11}$
CMOT	$2 \cdot 10^{10}$	$1 \cdot 10^{-3}$	$2 \cdot 10^{11}$
Gray Molasses	$1 \cdot 10^{10}$	$1 \cdot 10^{-4}$	$2 \cdot 10^{11}$

Table 2.3: Laser cooling performance.

after this will only show the atoms that are not hit by the beam. Figure 2-5(b) shows one of these images for a the gray molasses beam after aligning only with the center of the chamber, in which we can clearly see shells of atoms missed by the beam. After aligning the beam with the cloud using this image, we got an image of the missing part which looks like 2-5(c). We then repeat this procedure on all the beams as well as overlaping each pair of counter-propagating beams to make sure the gray molasses is well aligned with the CMOT cloud.

After we repeated this on all the gray molasses beams, we took time of flight images while scanning the frequencies of the light. As shown in figure 2-6, a clear decrease in temperature (a decrease in time of flight size) can be seen just as what we expected from the theory1.3.3 and the experimental results from other groups[2]. The final performance of the gray molasses is also listed in table 2.3. Since the gray molasses step does not provide spatial confinement, being able to maintain the same density as shown in the table confirms that the gray molasses can significantly cool the atoms before they fly away.

2.5 Dark State Pumping

At the end of Laser cooling, the atoms are distributed in different hyperfine levels not all of which are trappable in a magnetic trap. Therefore, in order to be trapped and evaporated in a magnetic trap, we need to transfer the atoms into either the $|F = 2, m_F = 2\rangle$ or $|F = 2, m_F = 1\rangle$ states which are trappable at both low field and
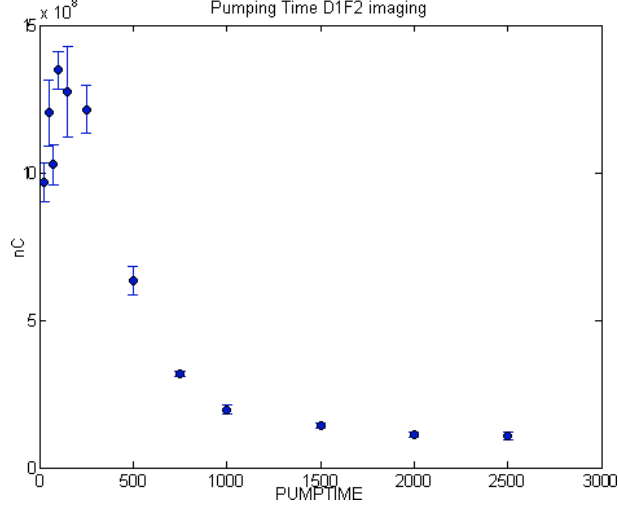
Figure 2-7: Atom number imaged with $D1(F = 2)$ σ^+ light as a function of dark state pumping time.

high field (). Moreover, for state preparation and minimizing inelastic collision rate, we use the streched $F = 2, m_F = 2$ state because it is pretected against spin-exchange collisions and therefore has a better elastic to inelastic collision rate ratio.

For transfering atom into the desired state, we use the technique known as dark state pumping to minimizing the heating from photon scattering during the pumping step. Using the $D1$ transition to the $F' = 2$ state, the $F = 2, m_F = 2$ state is dark for the σ^+ pumping light. In another word, after the atoms are pumped into the right state, they will become invisible and stop scattering any photons from the pump beam, in contrast with pumping with the $D2$ transition, in which case the atoms in the right state will cycle on the $F = 2, m_F = 2$ to $F' = 3, m'_F = 3$ and heats up quickly.

Another effect we want to avoid is the re-scattering of the pumping light, which happens when an atom goes into the $F = 2$ state and emit a photon close to resonance with the $F = 2$ transition with a random polarization that is not necessarily dark for the final state. Although it is believed that detuning the laser frequencies cannot reduce the re-scattering[3], we scan the laser powers and detunings of the pump light and find the best performance (shortest time and least heating) with maximum
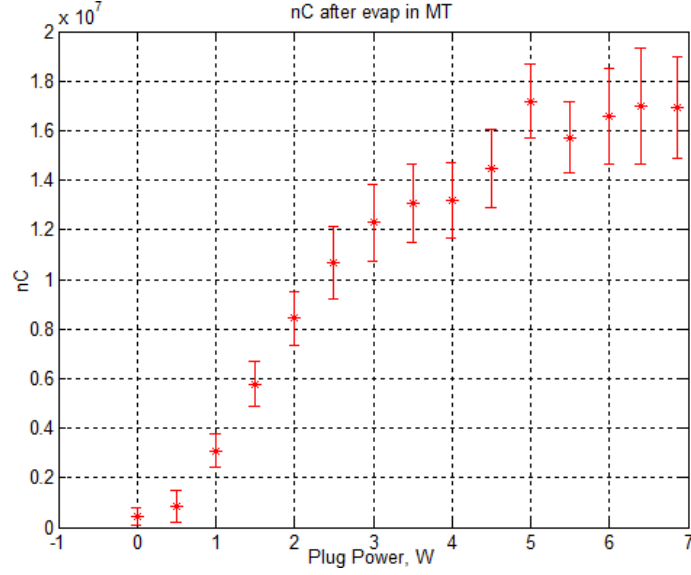
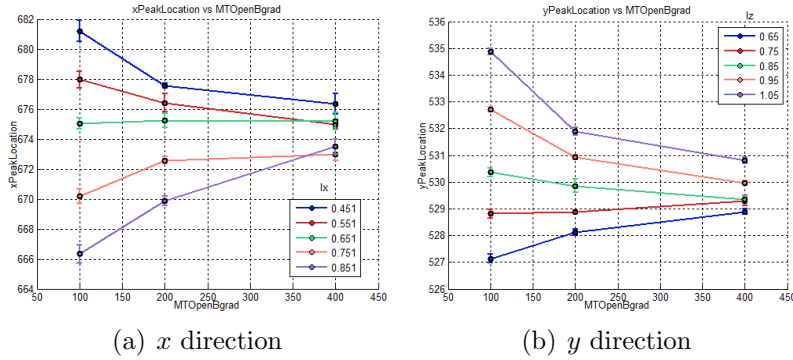Figure 2-8: Saturation of the Plug Laser Power.

(a) x direction   (b) y direction

Figure 2-9: Precise Field Zeroing in Magnetic trap

power and blue detuning of $\delta_{F1} = 20$MHz and $\delta_{F2} = 34$MHz for the $F1$ and $F2$ light respectively. Figure 2-7 shows the atoms after different pumping time imaged with $D1(F = 2)$ σ^+ light. The initial increase in atom number shows atoms being pumped into $F2$ and the slower decay is when they are going into the $|F = 2, m_F = 2\rangle$ state invisible to the imaging light.

2.6   Magnetic Trap

In order for an atom to stay trapped in a magnetic trap, it must maintain its Zeeman level. The adiabatic condition, tells us that this means the local magnetic field of an atom should not be too small or change too fast. Although this condition can be easily satisfied for a cold enough cloud, it cannot always hold around the center of the quadrupole magnetic trap where the field goes to zero. Therefore, there is a "hole" at the center of a quadrupole trap where atoms can spin flip and escape and the loss caused by this "hole" is called Majorana loss. Since the center of the trap is also the lowest point of the trapping potential and therefore is where the atom density is maximized, we will see large Majorana lossing rate in a pure quadrupole trap. The Majorana loss can be reduced or avoided by decreasing the atom number inside the hole. In our experiment, this is done with a "plug" beam which is a 10W 532nm green laser beam focused to $20\mu m$ at the center of the trap creating a positive AC Stark shift and pushing the atoms away from the center. Figure 2-8 shows the number of atom after the magnetic trap, the saturation of the atom number with 6W of plug power shows that we have successful suppressed the Majorana loss with the plug beam.

Due to the high three-body inelastic collision loss rate in Lithium-7, we need to open the trap, i.e. decrease the trapping gradient, during evaporation to keep a relatively low spatial density. However, since the center (zero) of the quadrupole field is determined by the ratio between the quadrupole field and the stray field around the center, the zero of the trap, therefore the Majorana hole, may move when we open the trap and might even move out of the plug beam. Although it is possible to shift either the zero or the plug and let them track each other during evaporation, the simplest way to solve the problem is actually to zero the stray field so that the center will never move while openning up. For achieving the high precision of field zeroing ($\leqslant$ 100mG), we zero the field by measuring the position of the center of the quadrupole trap. In the experiment, we decrease the trap gradient to certain value
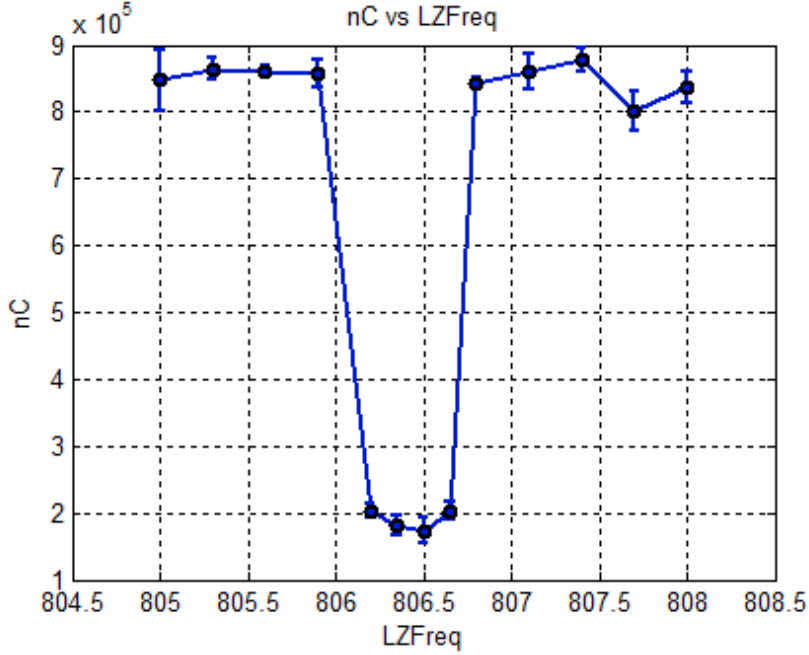
Figure 2-10: Atom number in $|F = 2, m_F = 2\rangle$ versus starting frequency of a 1MHz wide Landao-Zener sweep.

while doing a deep cut by sweeping the RF frequency close to resonance and measure the center position of the resulting small cloud left in the trap. Figure 2-9 shows the result of this measurement with different trap gradient and bias field in both x and y directions. We pick the bias field with the smallest displacement at different gradient, for which the center of the trap moves by smaller than one pixel ($20\mu m$).

Because of the small the elastic to inelastic collision rate ratio, the atom number fluctuation in the experiment and the necessity to open up the trap during evaporation, it is hard to optimize the RF evaporation purely experimentally. Instead, the evaporation in our experiment is optimized using numeric simulation. With our final sequence, after 2.5s of RF evaporation, we are left with $6 \cdot 10^7$ atoms with a temperature of $4\mu K$ and a density of $10^{12}cm^{-3}$.
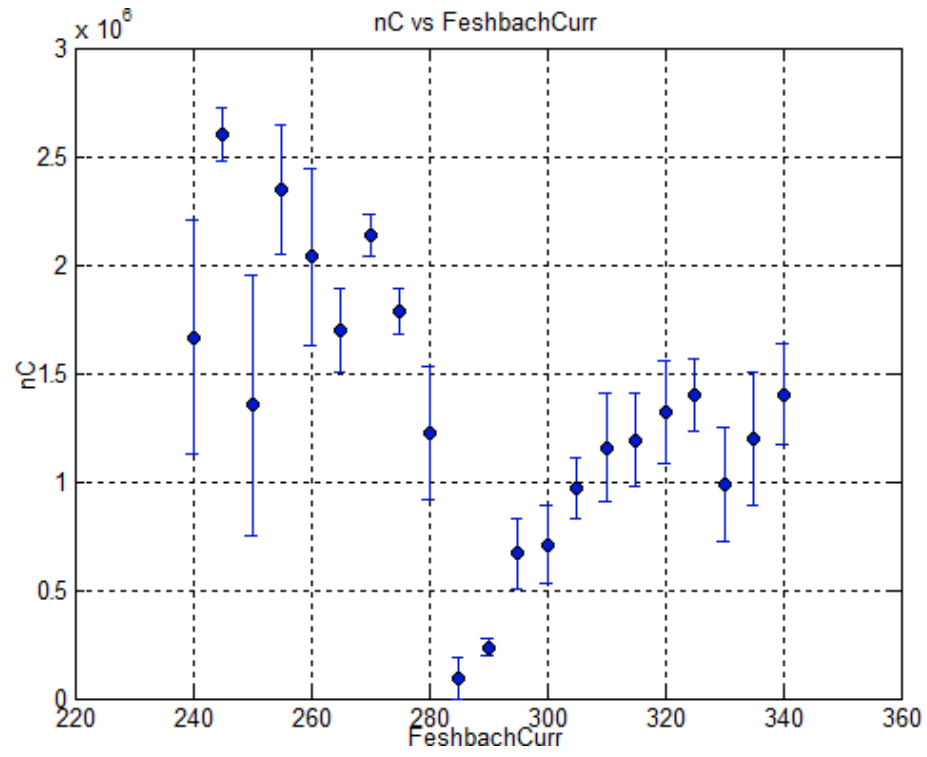
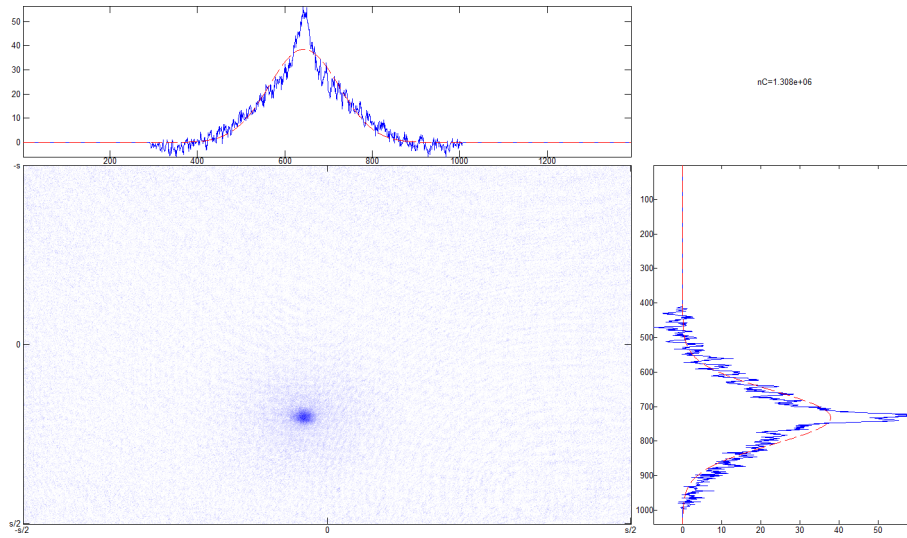Figure 2-11: Feshbach Resonance in $|F = 1, m_F = 1\rangle$ state.

Figure 2-12: BEC with thermal wing.

2.7   BEC in Optical Dipole Trap

After evaporation in the magnetic trap, we transfer the atoms into an optical dipole trap (ODT) created with two 15W 1064nm laser beams. This transfer need to be adiabatic in order to minimize heating and maximize transfer efficiency. After exploring different transfer schemes, the best method we have found is to turn on the ODT with full power before evaporating in the magnetic trap and ramp down the magnetic trap after evaporation in 200ms. In this way, we can accumulate $2 \cdot 10^7$ atoms in the ODT at a temperature of $20\mu K$.

We flip the atoms from $|F = 2, m_F = 2\rangle$ state to $|F = 1, m_F = 1\rangle$ state using a Landau-Zener sweep varying the RF frequency. Figure 2-10 shows the atom number in $|F = 2, m_F = 2\rangle$ versus starting frequency of a 1MHz wide RF scan in a magnetic field about 1.5G. We hit the resonance around 806.5MHz and the transfer efficiency is better than 80%. We believe the low effeciency of the transfer is mainly due to decoherence.

The evaporation in the ODT is aided by a Feshbach resonance, a resonance in the scattering length when the energy of a two-atom bound state matches the kinetic energy. In our experiment, this is achieved by adjusting the energy of the bound state with a magnetic field using Zeeman effect and is measured by observing the increase in three-body loss rate accompanied with the increase in scattering length. Figure 2-11 shows the atom number after a certain hold time in the ODT with different Feshbach fields. The resonance occurs at 285A (737G). By comparing the resonance point with know data for the scattering length around the resonance, we set the Feshbach field for our evaporation to $\approx 701G$ which corresponds to a reasonably large scattering length ($\approx 100a_0$). The evaporation is done by exponentially lower the ODT power, therefore the trapping depth, in each of the ODT beams from 15W to 1.5W over 250ms. The BEC we get after evaporation has an atom number of $5 \cdot 10^6$ at a temperature ≈ 100nK and condensate fraction $> 90\%$. By varying the evaporation

parameters, we are able to observe the BEC with different condensate fraction. Figure 2-12 is an image of a partially condenced BEC with a condensate fraction $\approx 15\%$.

Conclusion

The main goal of this work was to build an apparatus to experimentally realize a Bose-Einstein condensate of Lithium-7 which can be used as a starting point to study quantum magnetism in an optical lattice making use of the light mass and Feshbach resonance. The light mass, small elastic collision cross section and large inelastic collision loss of Lithium-7 poses challenges to both laser cooling and evaporative cooling. However, as shown in the previous chapter, using the non-conventional gray molasses cooling and numerically optimized RF evaporation, we have successfully archived our goal and are able to reach quantum degeneracy within 10 seconds including 6 seconds of MOT loading time. We have also measured the Feshbach resonance field which is important both for evaporation in ODT and for tuning interactions in a optical lattice.

Future work on this experiment will focus on characterizing and stabilizing our BEC and adding in the optical lattice in order to study solid state Hamiltonians we are interested in, including spin Hamiltonians for different phases of quantum magnetism.

Bibliography

[1] M. Fierz. über die relativistische theorie kräftefreier teilchen mit beliebigem spin. *Helvetica Physica Acta*, 1939.

[2] Andrew T. Grier, Igor Ferrier-Barbut, Benno S. Rem, Marion Delehaye, Lev Khaykovich, Frédéric Chevy, and Christophe Salomon. Λ-enhanced sub-doppler cooling of lithium atoms in $\mathbf{D}$1 gray molasses. *Phys. Rev. A*, 87:063411, Jun 2013.

[3] B. Lounis and C. Cohen-Tannoudji. Coherent population trapping and fano profiles. *J. Phys. II France*, 2:579–592, April 1992.

[4] W. Pauli. The connection between spin and statistics. *Phys. Rev.*, 58:716–722, 1940.

[5] Craig J. Sansonetti, C. E. Simien, J. D. Gillaspy, Joseph N. Tan, Samuel M. Brewer, Roger C. Brown, Saijun Wu, and J. V. Porto. Absolute transition frequencies and quantum interference in a frequency comb based measurement of the ^{6,7}**Li D** lines. *Phys. Rev. Lett.*, 107:023001, Jul 2011.

[6] D.S. Durfee W. Ketterle and D.M. Stamper-Kurn. Making, probing and understanding bose-einstein condensates. *In Bose-Einstein condensation in atomic gases, Proceedings of the International School of Physics "Enrico Fermi"*, pages 67–176, 1999.

[7] W. H. Wing. On neutral particle trapping in quasistatic electromagnetic fields. *Progress in Quantum Electronics*, 8:181–199, 1984.